



Current perspectives on the Permian–Triassic boundary and end-Permian mass extinction: Preface

Ian Metcalfe^{a,*}, Yukio Isozaki^b

^a School of Environmental and Rural Science, Earth Studies Building C02, University of New England, Armidale NSW 2351, Australia

^b Department of Earth Science and Astronomy, The University of Tokyo, 3-8-1 Komaba, Meguro, Tokyo 153-8902, Japan

ARTICLE INFO

Article history:

Received 14 July 2009

Accepted 18 July 2009

Keywords:

Permian–Triassic boundary

Mass extinction

Chemostratigraphy

Magnetostratigraphy

U–Pb zircon dating

Mantle plume

ABSTRACT

The end-Permian mass extinction is now robustly dated at 252.6 ± 0.2 Ma (U–Pb) and the Permian–Triassic (P–T) GSSP level is dated by interpolation at 252.5 Ma. An isotopic geochronological timescale for the Late Permian–Early Triassic, based on recent accurate high-precision U–Pb single zircon dating of volcanic ashes, together with calibrated conodont zonation schemes, is presented. The duration of the Early Triassic (Induan + Olenekian stages) is estimated at only 5.5 million years. The duration of the Induan Stage (Griesbachian + Dienerian sub-stages) is estimated at ca. one million years and the early Olenekian (Smithian sub-stage) at 0.7 million years duration. Considering this timescale, the “delayed” recovery following the end-Permian mass extinction may not in fact have been particularly protracted, in the light of the severity of the extinction. Conodonts evolved rapidly in the first 1 million years following the mass extinction leading to recognition of high-resolution conodont zones. Continued episodic global environmental and climatic stress following the extinction is recognized by multiple carbon isotope excursions, further faunal turnover and peculiar sedimentary and biotic facies (e.g. microbialites). The end-Permian mass extinction is interpreted to be synchronous globally and between marine and non-marine environments. The nature of the double-phased Late Permian extinction (at the Guadalupian–Lopingian boundary and the P–T boundary), linked to large igneous provinces, suggests a primary role for superplume activity that involved geomagnetic polarity change and massive volcanism.

© 2009 Elsevier Ltd. All rights reserved.

1. Introduction

The end-Permian extinction was arguably the most significant event in the past 600 million years of Earth’s history (Raup and Sepkoski, 1982; Sepkoski, 1984; Fig. 1). The loss of over 90% of all species brought the Palaeozoic Era to an end, reduced biological diversity for the following 25 million years of the early Mesozoic, and shaped the subsequent course of the evolution of life toward the present. The causes of this extinction are still in dispute.

The main end-Permian mass extinction pulse (much larger, and of greater effect on the evolution of life than the widely popularised Cretaceous–Palaeogene extinction that wiped out the dinosaurs) occurred just before the defined Permian–Triassic (P–T) Boundary (Yin et al., 2001; Metcalfe et al., 2001; Mundil et al., 2004). Arguments still rage over the duration and patterns of extinction, relative levels and temporal coincidence of extinctions in the sea and on land, and on causative mechanism(s). In addition, the significance of the end-Guadalupian extinction, another major

decline in biodiversity that took place ca. seven million years earlier (Jin et al., 1994; Stanley and Yang, 1994; Isozaki et al., 2004), has become more apparent as a precursor contribution to the severity of the end-Permian extinction. Furthermore, the nature, mechanisms and rates of biotic recovery following the extinction are likewise still poorly understood.

This special issue of the *Journal of Asian Earth Sciences* brings together a collection of papers that focus on these ongoing issues and which provide vital new data, constraints and interpretations relating to global biotic changes and turnover in the Late Permian and Early Triassic, a time when life nearly died on Earth. The topics include (1) pattern of faunal changes (Powers and Bottjer, 2009; Brayard et al., 2009), (2) stratigraphy and ecology of continental shelf (Chen et al., 2009; Mu et al., 2009), of mid-ocean (Isozaki, 2009; Horacek et al., 2009) and of terrestrial facies (Lucas, 2009; Metcalfe et al., 2009), and global correlation (Glen et al., 2009). As a background to these articles, we here present a brief introduction to current P–T Boundary studies, and in particular to provide an update on recent mass extinction-related topics. For further recent summaries and different aspects of P–T boundary issues the reader is referred to Erwin (2006) and Bottjer et al. (2008).

* Corresponding author.

E-mail address: imetcal2@une.edu.au (I. Metcalfe).

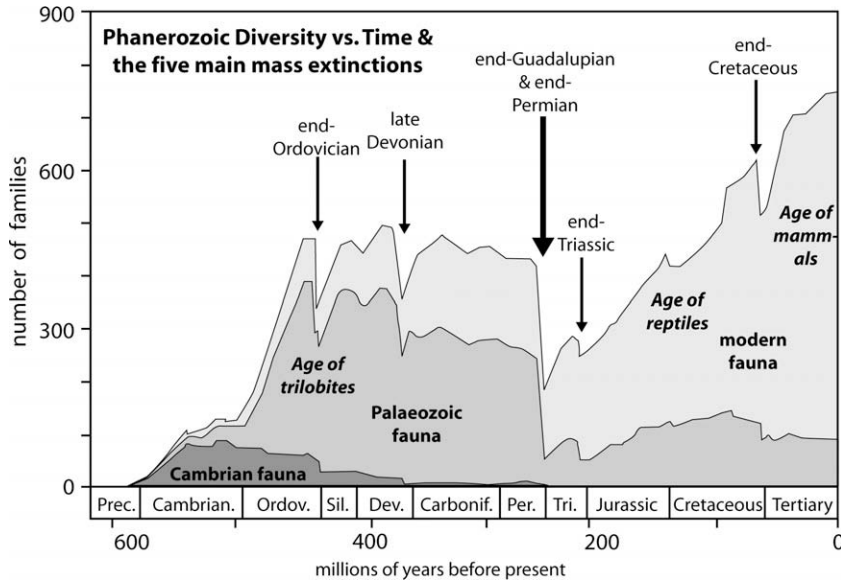


Fig. 1. Phanerozoic diversity vs. time plot showing the three major faunas and five major mass extinctions of the last 600 million years (after Sepkoski, 1984).

2. Timing and Tempo of extinction events and recovery

Dramatic improvements have been made in recent years on the Late Permian and Early Triassic timescale and on the timing and tempo of extinction events and recovery in this interval. The age of the end-Permian (latest Changhsingian) “mother of all” mass extinction is now robustly constrained by single crystal zircon closed-system U–Pb dating at 252.6 ± 0.2 Ma, and the currently defined base of the Triassic (P–T boundary) is interpolated as 252.5 ± 0.3 from bracketing ash bed dates (Mundil et al., 2004). The Global Stratotype Section and Point (GSSP) for the base of the Triassic (P–T boundary) at Meishan, China (Yin et al., 2001) is defined in shallow-marine strata (Fig. 2) by the first appearance of the conodont species *Hindeodus parvus* (Kozur and Pjatakova) in Bed 27c (Nicoll et al., 2002) and is dated at 252.5 ± 0.3 Ma based on zircon U–Pb analyses of bracketing ash beds (Mundil et al., 2001, 2004). The main end-Permian mass extinction level is at

the base of Bed 25 (Jin et al., 2000), 18 cm below the boundary. This level is dated at 252.6 ± 0.2 Ma by zircon U–Pb (Mundil et al., 2004). In other marine sections, the main mass extinction level may occur up to several meters below the biostratigraphically defined P–T boundary, or even several hundred meters below that level in thick continental deposits (e.g., Isozaki et al., 2007b; Metcalfe et al., 2009).

The age of the base of the Changhsingian stage, as interpolated from bracketing ash bed dates, is estimated at 256 Ma (Mundil et al., 2004). The base of the Wuchiapingian, and hence the age of the end-Guadalupian extinction, is not currently robustly constrained but estimated at ca. 260 Ma (Mundil et al., 2004; He et al., 2007). Recent single crystal U–Pb zircon dating of Lower Triassic volcanic ash beds in South China (Ovcharova et al., 2006; Lehrmann et al., 2006; Galfetti et al., 2007) provide important constraints on the ages of the Lower Triassic stage boundaries. Interpolation between accurate, high-precision U–Pb single zircon based

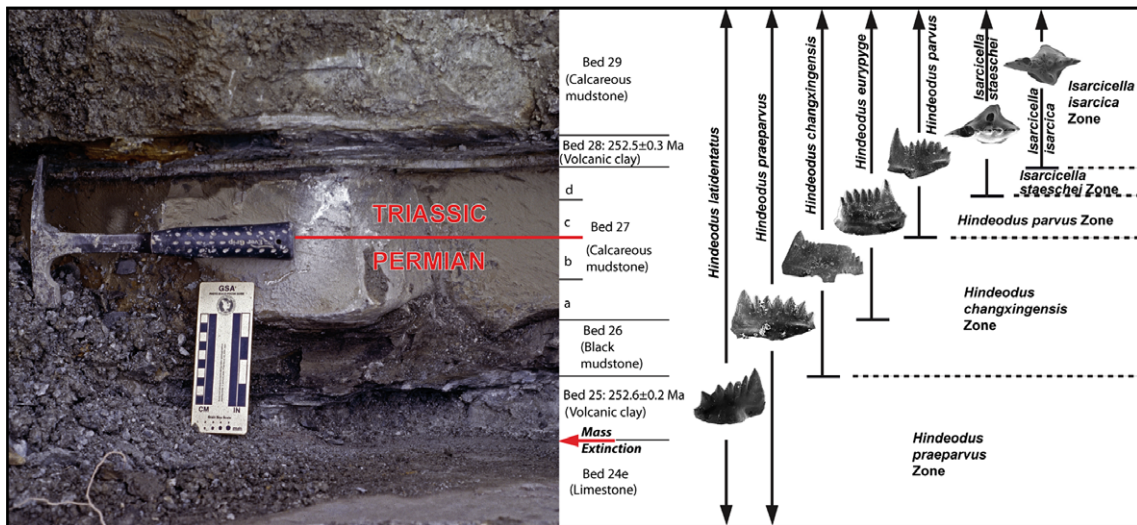


Fig. 2. Permian-Triassic boundary beds at the GSSP quarry D section, Meishan, China. Ages of mass extinction (Bed 25) and upper bracketing volcanic ash bed are from Mundil et al. (2001) and Mundil et al. (2004). Ranges of species of *Hindeodus* and *Isarcicella* (from Nicoll et al. (2002) and Jiang et al. (2007)) illustrate the rapid evolution of conodonts immediately following the mass extinction. Hindeodid zones are from Jiang et al. (2007).

ages of Mundil et al. (2004), Ovtcharova et al. (2006), Lehrmann et al. (2006) and Galfetti et al. (2007, see their Figs. 2 and 4) indicate that the age of the base of the Dienerian is 252 Ma, base Smithian is 251.5 Ma, base Spathian is 250.8 Ma and base Anisian is 247.2 Ma, respectively. The interpolation of these boundary ages is based on six robustly constrained Early Triassic ash bed ages in Guangxi, South China (Ovtcharova et al., 2006; Galfetti et al., 2007), four ash bed ages that straddle the Olenekian–Anisian boundary in the Guandao section, Guizhou (Lehrmann et al., 2006), and multiple Upper Permian–Lower Triassic ash bed ages at Meishan and Shangsi, South China (Mundil et al., 2004; Crowley et al., 2006) that are extremely well calibrated biostratigraphically. This new relatively robust timescale for the Late Permian–Early Triassic indicates that the entire Lower Triassic is only 5.3 million years in duration and that the earliest Triassic Induan stage (Griesbachian plus Dienerian sub-stages) is only ca. one million years in duration. The early Olenekian (Smithian substage) is also of very short duration at an estimated 0.7 million years, and the Upper Olenekian (Spathian substage) of relatively longer duration of 3.6 million years (see Fig. 3). The implications of this revised timescale are wide reaching for interpretations of P–T events and particularly for understanding recovery of biota following the extinction. The new timescale reported here suggests that the protracted

“delayed” recovery following the end-Permian mass extinction may not in fact have been so protracted, considering the severity of the extinction.

3. P–T boundary at GSSP and conodont zonation/correlation

The first appearance of *H. parvus* (Kozur and Pjatakova), used to recognise the base Triassic at the GSSP has proved to be very effective globally in precisely identifying this level in shallow-marine strata. In addition, high-resolution conodont biostratigraphy allows detailed correlation of both Upper Permian and Lower Triassic strata. There are however some major ongoing disagreements and debate relating to conodont taxonomy and conodont zones, particularly in the Upper Permian (e.g. Henderson et al., 2008) and there is ongoing debate as to the most suitable and globally applicable conodont zonations for the P–T transition (Fig. 3). Differences in taxonomic interpretations, faunal provincialism and possible homeomorphy of Upper Permian conodonts, coupled with possible miss-correlations of Changhsingian sections in Iran and between Iran and South China (Henderson et al., 2008) have led to problems of correlation of conodont zones and sequences of Tethys (Kozur, 2007) with the GSSP in South China (see Henderson et al., 2008 for detailed discussion). In addition to taxonomic differ-

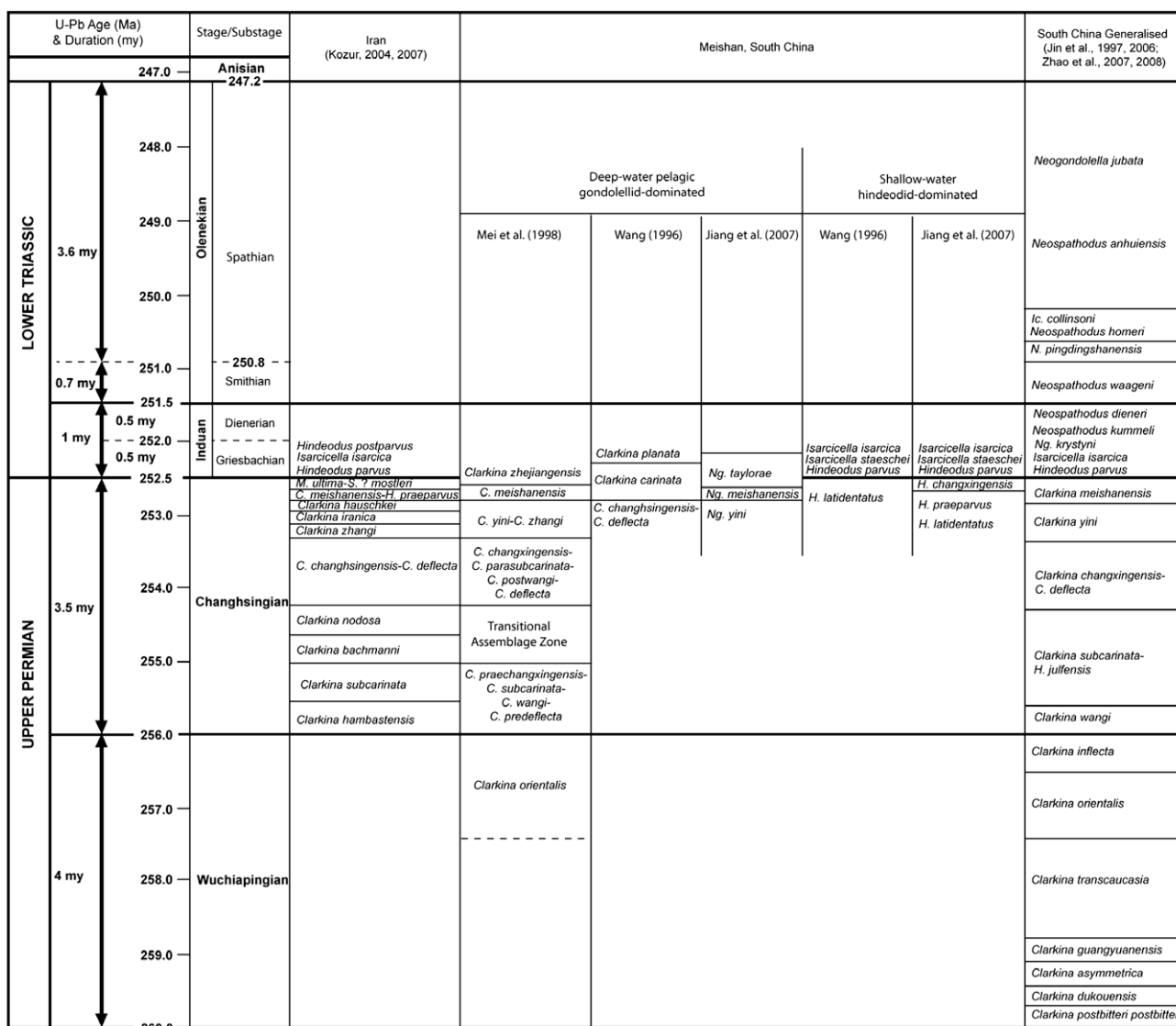


Fig. 3. Upper Permian–Lower Triassic timescale and correlation of conodont zones. See text for explanation. (See above-mentioned references for further information.)

ences, different zonal schemes for the P–T transition result from environmental/facies/depth influences leading, in particular, to zonations based on hindeodid-dominated or gondolellid-dominated conodont faunal successions (Jiang et al., 2007 – see Fig. 3). Chen et al. (2009) provides information on conodont biostratigraphy and zonation of the P–T transition by building on the taxonomic revision of the conodont genus *Hindeodus* by Nicoll et al. (2002) and by providing new data helping to distinguish between species and subspecies within the genus for enhanced conodont biozonation. Chen et al.'s correlation between the Great Bank of Guizhou and Meishan GSSP also demonstrates that the main end-Permian extinction is simultaneous in both sections and that the dissolution surface at the base of the calcimicrobialite at Dawen post-dates the extinction. We here present (Fig. 3) a correlation of P–T conodont zonal schemes in which we have attempted to account for the duration of specific conodont zones as far as possible within the P–T timescale we consider currently most robust. In doing this it is evident that in the latest Changhsingian to early Induan interval there are 6–8 conodont zones recognizable that represent about 1 million years compared with much longer duration conodont zones in the earlier part of the Late Permian and later part of the Early Triassic. This suggests rather rapid evolution and diversification of conodonts immediately following the main end-Permian mass extinction and includes what have been interpreted as “disaster species” such as *Hindeodus changhsingensis* Wang (Metcalfe et al., 2007).

4. Biotic and ecological changes

In addition to the traditional paleontological data, new lines of evidence for biotic and ecological changes across the boundary have become available from various sedimentary facies; e.g., peri-Pangean shallow marine shelf, deep and shallow mid-Panthalassa, and non-marine intra-Pangean basins. Continued harsh conditions in the immediate aftermath of the P–T extinction is suggested by faunal turnover and other sedimentary features in every facies. Powers and Bottjer (2009) document the distinct behavior of ligulid brachiopods that may suggest their physiological advantage for survival even among coeval lophophorates. One of the unique features also observed immediately after the P–T extinction horizon is the occurrence of microbialites in shallow marine settings both in Tethys and Panthalassa (Sano and Nakashima, 1997; Baud et al., 1997, 2005; Kershaw et al., 1999, 2002; Lehrmann, 1999; Lehrmann et al., 2003). This likewise recorded post-extinction deterioration of global environments with fewer metazoans but with abundant microbiota. Mu et al. (2009) add stable carbon isotope data to conclude that microbialites likely formed by upwelling of anoxic deep-water. During the Early Triassic, volatile fluctuation of C-isotopes, in accordance with biomarker evidence (Grice et al., 2005) was reported from peri-Pangean shelf carbonates (Payne et al., 2004), and Horacek et al. (2009) document an almost identical pattern in mid-oceanic carbonates from Panthalassa. Brayard et al. (2009) also show a good example of biotic response to climatic change of the Early Triassic ammonoid diversity gradients and their endemism. Isozaki (2009) summarizes the double-phased extinction pattern of dominant protists (radiolarians and fusulines) in deep and shallow mid-Panthalassa together with secular changes in C and Sr isotope ratios. Lucas (2009) reviews the extinction pattern of terrestrial tetrapods, whereas Metcalfe et al. (2009) demonstrate the almost synchronous extinction of terrestrial tetrapods in northern and southern hemispheres.

In recent times, attention has been diverted from the main end-Permian mass extinction to the end-Guadalupian extinction that occurred ca. seven million years earlier at c. 260 Ma. Details of the severity of this extinction compared to the end-Permian one are still largely lacking and more importantly, the role of the end

Guadalupian extinction as a precursor and contributor to the severity of the end-Permian extinction is poorly known. There is no doubt that many groups of organisms were severely weakened by the end Guadalupian extinction (Clapham et al., 2009) rendering them susceptible to annihilation during the end-Permian event ca. seven million years later.

5. Correlation of mass extinction level in marine, paralic and non-marine facies

Because the base Triassic GSSP is defined in a shallow-marine Tethyan sequence in the northern hemisphere, biostratigraphical correlation of this horizon and of the end-Permian mass extinction level a short distance below the boundary with non-marine terrestrial sequences globally and with high latitude southern hemisphere marine sequences has proved difficult. Proxy data for correlation of the P–T boundary and extinction levels include magnetostratigraphic data, chemostratigraphic data (especially stable carbon isotope data), radio-isotopic dating, and lithofacies/environmental and biotic change data that reflect changes in global climate. Lucas (2009) suggests that the tetrapod extinctions observed in the Permian–Triassic transitional interval are more gradual than previously thought and that these extinctions are not temporally coincident with the end-Permian main marine extinction. This is an important issue that impinges on identification of causative extinction mechanisms. We here suggest however that in fact the extinctions observed in the terrestrial environment in both northern and southern hemispheres (e.g. Dalongkou, Xinjiang, China: Metcalfe et al., 2009; and the Karoo Basin, South Africa: De Kock and Kirschvink, 2004; Ward et al., 2005; Coney et al., 2007) are temporally coincident and that these do in fact correlate in time with the mass extinction level in the marine environment (see below).

Magnetostratigraphy has great potential to effect robust global correlation through the P–T transition. Glen et al. (2009) report some vital new paleomagnetic data from marine, paralic and non-marine P–T sequences in China by demonstrating that the P–T boundary GSSP level falls within but near the base of a normal magnetic chron, and that the main end-Permian mass extinction level is at the base of that chron or just within the reversed chron below.

Chemostratigraphic correlation between marine and non-marine environments and between shallow Tethyan and deep Panthalassan sequences has great potential to provide important proxy correlations and also inform us on major global chemical changes in the oceans and atmosphere. Isozaki (2009) and Horacek et al. (2009) demonstrate that marine carbonate carbon isotope excursions observed in the Panthalassan realm do indeed mirror excursions documented elsewhere in the shallow-marine environment globally. What is not so clear is whether organic carbon isotope excursions documented from terrestrial sequences can be precisely correlated with carbonate carbon isotope excursions of the marine environment. Metcalfe et al. (2009) present lithostratigraphical, biostratigraphical, and carbon isotope data from the important terrestrial sequence at Dalongkou in the Jungar Basin, China. The carbon isotope data indicate two broad negative excursions in the Guodikeng Formation, which has recently been confirmed by parallel studies (Cao et al., 2008) and these appear to correlate with the double late Changhsingian excursions seen in the shallow-marine environment (Fig. 13 of Metcalfe et al., 2009; Fig. 2 of Cao et al., 2008).

An ongoing issue that impacts on identifying causative mechanisms for the end-Permian mass extinction is the question of any variability in the timing of the extinction. Is the extinction synchronous or diachronous between marine and non-marine environments or between different geographic regions? Wignall and

Newton (2003) suggested that the extinction is diachronous between Tibet and British Columbia in moderately deep marine environments based mainly on variability of the onset of euxinia. However, more recent biostratigraphic work on the Selong section in Tibet (Shen et al., 2006) and Canadian sections demonstrate that there is unlikely to be any age difference in the mass extinction level. Recent studies and correlations between marine, paralic and terrestrial P–T sequences in China also suggest that the mass extinction is synchronous between these sequences (Peng et al., 2005; Metcalfe and Nicoll, 2007). A recent preliminary U–Pb single crystal zircon age of 252.2 ± 0.4 Ma from very close to the interpreted mass extinction level in the Bowen Basin, Australia (Mundil et al., 2006) suggests that there is essentially no difference in age between the mass extinction level in the terrestrial sequences of Australian Gondwana and the shallow-marine GSSP section in China. Correlations of terrestrial sequences in the Karoo Basin, Africa with the rest of the world (e.g. Ward et al., 2005), including a single crystal U–Pb zircon age of 252.5 ± 0.7 Ma from the mass extinction horizon in the Commando Drift Dam section (Coney et al., 2007) again suggest that the end-Permian mass extinction is synchronous globally, both in the oceans and on land. The synchronicity of mass extinction in both marine and terrestrial environments has major implications for constraining proposed causative mechanisms.

6. Double-phased extinction and its causative mechanism(s)

We do not intend to discuss in detail the various competing hypotheses for the end-Permian (or end-Guadalupian) mass extinction here. Nonetheless, as all the putative bolide/cometary-impact explanations appear quite unlikely, the most popular at present are scenarios that link flood basalt volcanism (e.g. Siberian Traps, Emeishan Traps) and extinction (e.g., Campbell et al., 1992; Chung et al., 1998; Courtillot, 1999; Wignall et al., 2009). With recent robust demonstration of temporal coincidence between LIPs and the end-Guadalupian and end-Permian extinctions (e.g. Zhou et al., 2002; Mundil et al., 2004; He et al., 2007), and interpretations from carbon isotope records, the primary role of massive volcanism seems convincing.

On the basis of new data from the superocean Panthalassa Isozaki (2009), discusses the double-phased Late Permian extinction with respect to the waxing/waning of the superanoxic conditions in the deep marine environment during the Permian–Triassic transition and links these to the temporally coincident formation of Large Igneous Provinces (LIPs). He further suggests that the launching of a superplume from the core-mantle boundary may have triggered decay of the Earth's magnetic field at the end of the Kiaman Reverse Superchron (ca. 265 Ma) to allow much stronger cosmic radiation and to start cooling on the planet's surface (e.g. Kamura cooling event, Isozaki et al., 2007a). The responsible superplume consequently impinged beneath Pangea to start violent volcanism with biosphere perturbation (global plume winters) followed by global warming (plume summers) coupled with major atmospheric compositional changes and anoxia.

What is not so clear perhaps is the secondary role of other potential causative mechanisms and much work remains to unequivocally demonstrate the ultimate causes of the end-Permian devastation of life.

Note added in proof

An article by Korte et al. entitled “Massive volcanism at the Permian–Triassic boundary and its impact on the isotopic composition of the ocean and atmosphere” was originally planned to be included in this special issue but due to delay in revision it will appear in a succeeding normal issue.

Acknowledgments

We greatly appreciate the editorial work undertaken by our Editor-in Chief Borming Jahn and Editorial Assistants Jennifer Leong and Alan Arevalo for this special issue. This issue is a contribution to IGCP 572 “Permian–Triassic ecosystems”.

References

- Baud, A., Cirilli, S., Marcoux, J., 1997. Biotic response to mass extinction: the lowermost Triassic microbialites. *Facies* 36, 238–242.
- Baud, A., Richoz, S., Marcoux, J., 2005. Calcimicrobial cap rocks from the basal Triassic units: western Taurus occurrences (SW Turkey). *Comptes Rendus Palevol* 4, 501–514.
- Bottjer, D.J., Clapham, M.E., Fraiser, M.L., Powers, C.M., 2008. Understanding mechanisms for the end-Permian mass extinction and the protracted Early Triassic aftermath and recovery. *GSA Today* 18, 4–10.
- Brayard, A., Escarguel, G., Bucher, H., Bruhwiler, T., 2009. Smithian and Spathian (Early Triassic) ammonoid assemblages from terranes: paleoceanographic and paleogeographic implications. *Journal of Asian Earth Sciences* 36, 420–433.
- Campbell, I., Czamanske, G.K., Fedorenko, V.A., Hill, R.L., Stepanov, V., 1992. Synchronism of the Siberian traps and the Permian–Triassic boundary. *Science* 258, 1760–1763.
- Cao, C., Wang, W., Liu, L., Shen, S., Summons, R.E., 2008. Two episodes of ^{13}C -depletion in organic carbon in the latest Permian: Evidence from the terrestrial sequences in northern Xinjiang, China. *Earth and Planetary Science Letters* 270, 251–257.
- Chen, J., Beatty, T.W., Henderson, C.M., Rowe, H., 2009. Conodont biostratigraphy across the Permian–Triassic boundary at the Dawen section, Great Bank of Guizhou, Guizhou Province, South China: Implications for the Late Permian extinction and correlation with Meishan. *Journal of Asian Earth Sciences* 36, 442–458.
- Chung, S.L., Jahn, B.M., Wu, G.Y., Lo, C.H., Cong, B.L., 1998. The Emeishan flood basalt in SW China: a mantle plume initiation model and its connection with continental breakup and mass extinction at the Permian–Triassic boundary. *American Geophysical Union Geodynamic Series* 27, 47–58.
- Clapham, M.E., Shen, S.Z., Bottjer, D.J., 2009. The double mass extinction revisited: reassessing the severity, selectivity, and causes of the end-Guadalupian biotic crisis (Late Permian). *Palaeobiology* 35, 32–50.
- Coney, L., Reimold, W.U., Hancox, P.J., Mader, D., Koeberl, C., McDonald, I., Struck, U., Vajda, V., Kamo, S.L., 2007. Geochemical and mineralogical investigation of the Permian–Triassic boundary in the continental realm of the southern Karoo Basin, South Africa. *Palaeoworld* 16 (2007), 67–104.
- Courtillot, V., 1999. *Evolutionary Catastrophe*. Cambridge Univ. Press, Cambridge, p. 173.
- Crowley, J.L., Bowring, S.A., Shen, S.Z., Wang, Y., Cao, C., Jin, Y.G., 2006. U–Pb zircon geochronology of the end-Permian mass extinction. In: 16th Goldschmidt Conference Melbourne (Abstracts, A119).
- De Kock, M.O., Kirschvink, J.L., 2004. Paleomagnetic constraints on the Permian–Triassic boundary in Terrestrial Strata of the Karoo Supergroup, South Africa: implications for causes of the end-Permian extinction event. *Gondwana Research* 7, 175–183.
- Erwin, D.H., 2006. *Extinction. How Life on Earth Nearly Ended 250 Million Years Ago*. Princeton University Press, Princeton, Oxford, ix + 296 pp.
- Galfetti, T., Bucher, H., Ovtcharova, M., Schaltegger, U., Brayard, A., Bruhwiler, T., Goudemand, N., Weissert, H., Hochuli, P.A., Cordey, F., Guodun, K., 2007. Timing of the Early Triassic carbon cycle perturbations inferred from new U–Pb ages and ammonoid biochronozones. *Earth and Planetary Science Letters* 258, 593–604.
- Glen, J.M.G., Nomade, S., Lyons, J.J., Metcalfe, I., Mundil, R., Renne, P.R., 2009. Magnetostratigraphic correlations of Permian–Triassic marine and terrestrial sediments from western China. *Journal of Asian Earth Sciences* 36, 521–540.
- Grice, K., Cao, C., Love, G.D., Böttcher, M.E., Twitchett, R.J., Grosjean, E., Summons, R.E., Turgeon, S.C., Dunning, W., Jin, Y., 2005. Photic Zone Euxinia During the Permian–Triassic Superanoxic Event. *Science* 307, 706–709.
- He, B., Xu, Y.G., Huang, X.L., Luo, Z.Y., Shi, Y.R., Yang, Q.J., Yu, S.Y., 2007. Age and duration of the Emeishan flood volcanism, SW China: geochemistry and SHRIMP zircon U–Pb dating of silicic ignimbrites, post-volcanic Xuanwei formation and clay tuff at the Chaotian section. *Earth and Planetary Science Letters* 255, 306–323.
- Henderson, C.M., Mei, S.L., Shen, S.Z., Wardlaw, B.R., 2008. Resolution of the reported Upper Permian conodont occurrences from northwestern Iran. *Permian* 51, 2–9.
- Horacek, M., Koike, T., Richoz, S., 2009. Lower Triassic ^{13}C isotope curve from shallow-marine carbonates in Japan, Panthalassa realm: confirmation of the Tethys $\delta^{13}\text{C}$ curve. *Journal of Asian Earth Sciences* 36, 481–490.
- Isozaki, Y., 2009. Integrated plume winter scenario for the double-phased extinction during the Paleozoic–Mesozoic transition: the G-LB and P-TB events from a Panthalassan perspective. *Journal of Asian Earth Sciences* (this issue). doi:10.1016/j.jseas.2008.05.006.
- Isozaki, Y., Kawahata, H., Ota, A., 2007a. A unique carbon isotope record across the Guadalupian–Lopingian (Middle–Upper Permian) boundary in mid-oceanic

- paleoatoll carbonates: the high-productivity "Kamura event" and its collapse in Panthalassa. *Global and Planetary Change* 55, 21–38.
- Isozaki, Y., Shimizu, N., Yao, J.X., Ji, Z.S., Matsuda, T., 2007b. The end-Permian extinction and volcanism-induced environmental stress: Permo-Triassic boundary interval of a lower slope facies at Chaotian, South China. *Palaeogeography Palaeoclimatology Palaeoecology* 252, 218–238.
- Isozaki, Y., Yao, J.X., Matsuda, T., Sakai, H., Ji, Z.S., Shimizu, N., Kobayashi, N., Kawahata, H., Nishi, H., Takano, M. and Kubo, T., 2004. Stratigraphy of the Middle-Upper Permian and Lowermost Triassic at Chaotian, Sichuan, China – Record of Late Permian double mass extinction events. *Proceedings of Japan Academy* 80B, 10–16.
- Jiang, H.S., Lai, X.L., Luo, G.M., Aldridge, R., Zhan, K.X., Wignall, P.B., 2007. Restudy of conodont zonation and evolution across the P/T boundary at Meishan section, Changxing, Zhejiang, China. *Global and Planetary Change* 55, 39–55.
- Jin, Y.G., Zhang, J., Shang, Q.H., 1994. Two phases of the end-Permian mass extinction. In: Embry, A.F., Beauchamp, B., Glass, D.J., (Eds.), *Pangea: Global Environments and Resources*, Memoir Canadian Society of Petroleum Geologists, vol. 17, pp. 813–822.
- Jin, Y.G., Wardlaw, B.R., Glenister, B.F., Kotlyar, G.V., 1997. Permian chronostratigraphic subdivisions. *Episodes* 20, 10–15.
- Jin, Y.G., Wang, Y., Wang, W., Shang, Q.H., Cao, C.Q., Erwin, D.H., 2000. Pattern of marine mass extinction near the Permian-Triassic boundary in South China. *Science* 289, 432–436.
- Jin, Y.G., Wang, Y., Henderson, C., Wardlaw, B.R., Shen, S., Cao, C., 2006. The global boundary stratotype section and point (GSSP) for the base of Changhsingian stage (Upper Permian). *Episodes* 29, 175–182.
- Kershaw, S., Zhang, T.S., Lan, G.Z., 1999. A microbialite carbonate crust at the Permian-Triassic boundary in South China, and its palaeoenvironmental significance. *Palaeogeography, Palaeoclimatology, Palaeoecology* 146, 1–18.
- Kershaw, S., Guo, L., Swift, A., Fan, J., 2002. Microbialites in the Permian-Triassic boundary interval in central China: structure, age and distribution. *Facies* 47, 83–89.
- Kozur, H.W., 2007. Biostratigraphy and event stratigraphy in Iran around the Permian-Triassic boundary (PTB); implications for the causes of the PTB biotic crisis. Environmental and biotic changes during the Paleozoic-Mesozoic transition. *Global and Planetary Change* 55, 155–176.
- Lehrmann, D.J., 1999. Early Triassic calcimicrobial mounds and biostromes of the Nanpanjiang basin, south China. *Geology* 27, 359–362.
- Lehrmann, D.J., Payne, J.L., Felix, S.V., Dillett, P.M., Wang, H., Yu, Y.Y., Wei, J.Y., 2003. Permian-Triassic boundary sections from shallow-marine carbonate platforms of the Nanpanjiang Basin, south China: implications for oceanic conditions associated with the end-Permian extinction and its aftermath. *Palaios* 18, 138–152.
- Lehrmann, D.J., Ramezani, J., Bowring, S.A., Martin, M.W., Montgomery, P., Enos, P., Payne, J.L., Orchard, M.J., Wang, H., Wei, J.Y., 2006. Timing of recovery from the end-Permian extinction: geochronologic and biostratigraphic constraints from South China. *Geology* 34, 1053–1056.
- Lucas, S.G., 2009. Timing and magnitude of tetrapod extinctions across the Permo-Triassic boundary. *Journal of Asian Earth Sciences* 36, 491–502.
- Mei, S.L., Zhang, K.X., Wardlaw, B.R., 1998. A refined succession of Changhsingian and Griesbachian neogondolellid conodonts from the Meishan section, candidate of the global stratotype section and point of the Permian-Triassic boundary. *Palaeogeography, Palaeoclimatology, Palaeoecology* 143, 213–226.
- Metcalfe, I., Foster, C.B., Afonin, S.A., Nicoll, R.S., Mundil, R., Wang, X.F., Lucas, S.G., 2009. Stratigraphy, biostratigraphy and C-isotopes of the Permian-Triassic non-marine sequence at Dalongkou and Lucaogou, Xinjiang Province, China. *Journal of Asian Earth Sciences* 36, 503–520.
- Metcalfe, I., Nicoll, R.S., 2007. Conodont biostratigraphic control on transitional marine to non-marine Permian-Triassic boundary sequences in Yunnan-Guizhou, China. *Palaeogeography Palaeoclimatology Palaeoecology* 252, 56–65.
- Metcalfe, I., Nicoll, R.S., Mundil, R., Foster, C., Glen, J., Lyons, J., Wang, X.F., Wang, C.Y., Renne, P.R., Black, L., Qu, X., Mao, X.D., 2001. The Permian-Triassic boundary and mass extinction in China. *Episodes* 24 (4), 239–244.
- Metcalfe, I., Nicoll, R.S., Wardlaw, B.R., 2007. Conodont index fossil *Hindeodus changhsingensis* Wang fingers greatest mass extinction event. *Palaeoworld* 16, 202–207.
- Mu, X., Kershaw, S., Li, Y., Guo, L., Qi, Y., Reynolds, A., 2009. High-resolution carbon isotope changes in the Permian-Triassic boundary interval, Chongqing, South China; implications for control and growth of earliest Triassic microbialites. *Journal of Asian Earth Sciences* 36, 434–441.
- Mundil, R., Metcalfe, I., Ludwig, K.R., Renne, P.R., Oberli, F., Nicoll, R.S., 2001. Timing of the Permian-Triassic biotic crisis: implications from new zircon U/Pb age data (and their limitations). *Earth and Planetary Science Letters* 187, 131–145.
- Mundil, R., Ludwig, K.R., Metcalfe, I., Renne, P.R., 2004. Age and timing of the Permian mass extinctions: U/Pb geochronology on closed-system zircons. *Science* 305, 1760–1763.
- Mundil, R., Metcalfe, I., Chang, S., Renne, P.R., 2006. The Permian-Triassic boundary in Australia: New radio-isotopic ages. In: 16th Goldschmidt Conference Melbourne, Awards ceremony speeches and abstracts, p. A436. *Geochimica et Cosmochimica Acta* 70 (18) (Suppl. 1).
- Nicoll, R.S., Metcalfe, I., Wang, C.Y., 2002. New species of the conodont Genus *Hindeodus* and the conodont biostratigraphy of the Permian-Triassic boundary interval. *Journal of Asian Earth Sciences* 20, 609–631.
- Ovtcharova, M., Bucher, H., Schaltegger, U., Galfetti, T., Brayard, A., Guex, J., 2006. New Early to Middle Triassic U-Pb ages from South China: calibration with ammonoid biochronozones and implications for the timing of the Triassic biotic recovery. *Earth and Planetary Science Letters* 243, 463–475.
- Payne, J.L., Lehrmann, D.J., Wei, J., Orchard, M.J., Schrag, D.P., Knoll, A.H., 2004. Large perturbations of the carbon cycle during recovery from the end-Permian mass extinction. *Science* 305, 506–509.
- Peng, Y., Zhang, S., Yu, T., Yang, F., Gao, Y., Shi, G.R., 2005. High resolution terrestrial Permian-Triassic eventostratigraphic boundary in western Guizhou and eastern Yunnan, southwestern China. *Palaeogeography, Palaeoclimatology, Palaeoecology* 215, 285–295.
- Powers, C.M., Bottjer, D.J., 2009. Behavior of lophophorates during the end-Permian mass extinction and recovery. *Journal of Asian Earth Sciences* 36, 413–419.
- Raup, D.M., Sepkoski Jr., J.J., 1982. Mass extinctions in the marine fossil record. *Science* 215, 1501–1503.
- Sano, H., Nakashima, K., 1997. Lowermost Triassic (Griesbachian) microbial bindstone-cementstone facies, southwest Japan. *Facies* 36, 1–24.
- Sepkoski Jr., J.J., 1984. A kinetic model of Phanerozoic taxonomic diversity. III. Post-Paleozoic families and mass extinction. *Paleobiology* 10, 246–267.
- Shen, S.Z., Cao, C.Q., Henderson, C.M., Wang, X.D., Shi, G.R., Wang, Y., Wang, W., 2006. End-Permian mass extinction pattern in the northern peri-Gondwanan region. *Palaeoworld* 15, 3–30.
- Stanley, S.M., Yang, X., 1994. A double mass extinction at the end of the Paleozoic era. *Science* 266, 1340–1344.
- Wang, C., 1996. Conodont evolutionary lineage and zonation for the Latest Permian and the Earliest Triassic. *Permophiles* 29, 30–37.
- Ward, P.J., Botha, J., Buick, R., De Kock, M.O., Erwin, D.H., Garrison, G.H., Kirschvink, J.L., Smith, R., 2005. Abrupt and gradual extinction among late Permian land vertebrates in the Karoo Basin, South Africa. *Science* 307, 709–714.
- Wignall, P.B., Newton, R., 2003. Contrasting deep-water records from the Upper Permian and Lower Triassic of South Tibet and British Columbia: evidence for a diachronous mass extinction. *Palaios* 18, 153–167.
- Wignall, P.B., Sun, Y., Bond, D.P.G., Izon, G., Newton, R.J., Védrine, S., Widdowson, M., Ali, J.R., Lai, X., Jiang, H., Cope, H., Bottrell, S.H., 2009. Volcanism, mass extinction, and carbon isotope fluctuations in the Middle Permian of China. *Science* 324, 1179–1182.
- Yin, H.F., Zhang, K.X., Tong, J.N., Yang, Z.Y., Wu, S.B., 2001. The global stratotype section and point (GSSP) of the Permian-Triassic boundary. *Episodes* 24, 102–114.
- Zhao, L.S., Orchard, M.J., Tong, J.N., Sun, Z.M., Zuo, J.X., Zhang, S.X., Yun, A.L., 2007. Lower Triassic conodont sequence in Chaohu, Anhui Province, China and its global correlation. *Palaeogeography, Palaeoclimatology, Palaeoecology* 252, 24–38.
- Zhao, L.S., Tong, J.N., Sun, Z.M., Orchard, M.J., 2008. A detailed Lower Triassic conodont biostratigraphy and its implications for the GSSP candidate of the Induan-Olenekian boundary in Chaohu, Anhui province. *Progress in Natural Science* 18, 79–90.
- Zhou, M.F., Malpas, J., Song, X.Y., Robinson, P.T., Sun, M., Kennedy, A.K., Leshner, C.M., Keays, R.R., 2002. A temporal link between the Emeishan large igneous province (SW China) and the end-Guadalupian mass extinction. *Earth and Planetary Science Letters* 196, 113–122.